Magnetic Resonance in Medicine 47:696–700 (2002)
DOI 10.1002/mrm.10114

Fast Maximum Intensity Projection Algorithm Using Shear Warp Factorization and Reduced Resampling

Laifa Fang,[1,2] Yi Wang,[3*] Bensheng Qiu,[1] and Yuancheng Qian[2]

Maximal intensity projection (MIP) is routinely used to view MRA and other volumetric angiographic data. The straightforward implementation of MIP is ray casting that traces a volumetric data set in a computationally expensive manner. This article reports a fast MIP algorithm using shear warp factorization and reduced resampling that drastically reduced the redundancy in the computations for projection, thereby speeding up MIP by more than 10 times. Magn Reson Med 47:696–700, 2002.

Key words: MIP; maximal intensity projection; shear warp factorization; reduced resampling

Maximum intensity projection (MIP) is the most widely used algorithm for displaying volumetric angiographic data in MRI and CT (1–6). A brute force method for implementing MIP is ray casting and searching for the maximal intensity in that ray (7). The computation cost consists of addressing the data storage and resampling data along a ray. Because addressing arithmetic has to be performed for each ray, the computation becomes expensive for the large datasets typically associated with high-resolution angiographic data. The shear warp factorization method has been developed to minimize the amount of addressing arithmetic required for ray casting in volume rendering (8–11). Recently, this shear warp factorization has also been adapted to speed up projections in MIP based on nearest neighbor approximation (12). In this study, we developed the shear warp factorized MIP using linear interpolation, which is more accurate than the nearest neighbor approximation (13). We also introduced a reduced resampling method to further reduce the redundancy in computation. We evaluated our fast MIP algorithm on volumetric time of flight and contrast-enhanced magnetic resonance angiography (MRA) data.

METHODS

Ray Casting and Shear Warp

For reference, the ray casting method is illustrated in Fig. 1. The shear warp factorization method is illustrated in Fig. 2. The shear warp factorization method operates by factorizing the viewing transformation matrix into a 3D shear parallel to the data slices to form an intermediate but distorted projection image and then applying a 2D warp to form an undistorted final image (11). For affine viewing transformation matrix (M_{view}) concerned in this study, the shear warp factorization includes a permutation (represented by matrix P), a 3D shear (represented by matrix M_{shear}), and a 2D warp (represented by matrix M_{warp}): $M_{view} = M_{warp}M_{shear}P$. The permutation matrix P is associated with the choice of the principal viewing axis. The geometry specified by the viewing matrix M_{view} determines the shear matrix M_{shear} and the warp matrix M_{warp} (only a 2D warp matrix is needed). The details for the calculation of M_{shear} and M_{warp} from a given M_{view} can be found in Ref. 11 and are summarized in the Appendix.

This shear warp factorization allows substantial reduction of computation cost, which we demonstrate here for the case of linear interpolation. The computation for trilinear resampling in ray casting (Fig. 1b) is:

$$V_{xyz} = \sum_{i=0}^{1}\sum_{j=0}^{1}\sum_{k=0}^{1}(1-|x-i|)(1-|y-j|)(1-|z-k|)V_{ijk}. \quad [1]$$

Here V_{xyz} is the interpolated value for the ray point (x,y,z) in the cell and V_{ijk} is the image intensity value at cell corner (i,j,k). There are a total of $3 \times 8 = 24$ multiplications. Note that the symmetry in the weighting coefficients in Eq. [1] allows reduction of another four multiplications. Accordingly, the resampling computation cost per cell is approximately 20 multiplications.

Similarly, the computation for the bilinear resampling in shear warp factorization (Fig. 2b) is:

$$V_{xy} = \sum_{i=0}^{1}\sum_{j=0}^{1}(1-|x-i|)(1-|y-j|)V_{ij}. \quad [2]$$

There are a total of $2 \times 4 = 8$ multiplications. Note that the weighting coefficients are the same for all cells in a slice (Fig. 2). Accordingly, the multiplication for the weighting coefficients in Eq. [2] can be done once at the beginning for each projection and the resampling computation cost per cell is approximately four multiplications. Compared to ray casting (Eq. 1), the shear warp factorization reduces the computation time by approximately five times.

Another benefit of the shear warp algorithm is that it accesses the volume data in storage order (slice after slice), therefore simplifying the tedious addressing calculation that is needed in the ray casting algorithm. This efficient traversing through the volume data boosts projection speed. However, the shear direction may be one of the three orthogonal axes depending on the projection angle. In our implementa-

[1]PLA General Hospital, Beijing, China.
[2]Hefei University of Technology, Anhui Province, China.
[3]Weill Medical College of Cornell University, New York, New York.
Grant sponsors: Chinese National Science Foundation; US Department of Public Health Service; Grant numbers: R01HL60879; R01HL62994.
*Correspondence to: Yi Wang, Ph.D., MR Research Center, B-864, UPMC Presbyterian, 200 Lothrop St., Pittsburgh, PA 15213.
E-mail: wang@mrctr.upnc.edu
Received 20 August 2001; revised 29 November 2001; accepted 30 November 2001.

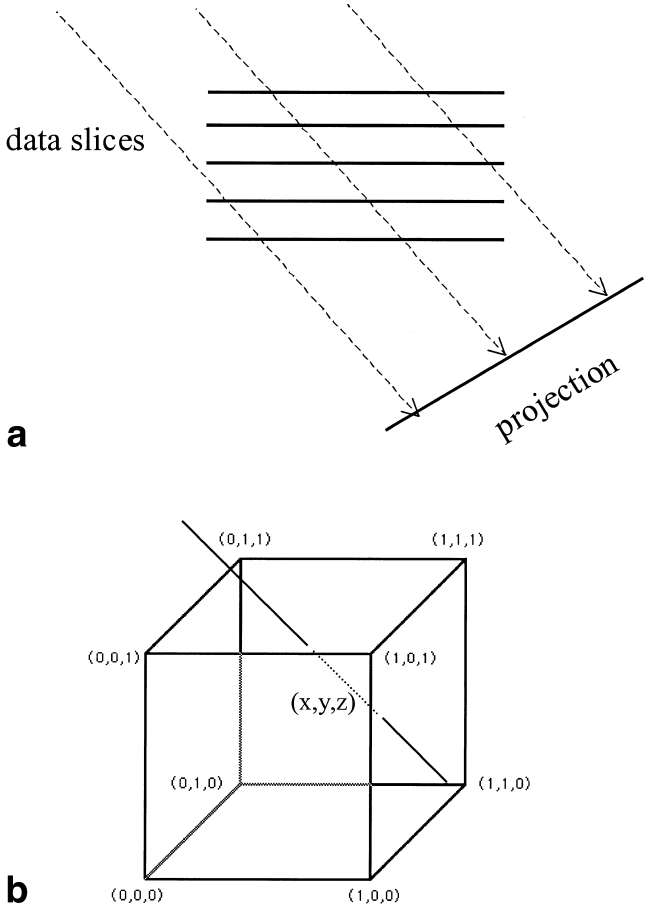

FIG. 1. Schematics (**a**) and one cubic resampling cell along a ray (**b**) of ray casting. The coordinates for the point on a ray and the eight cell corners are labeled.

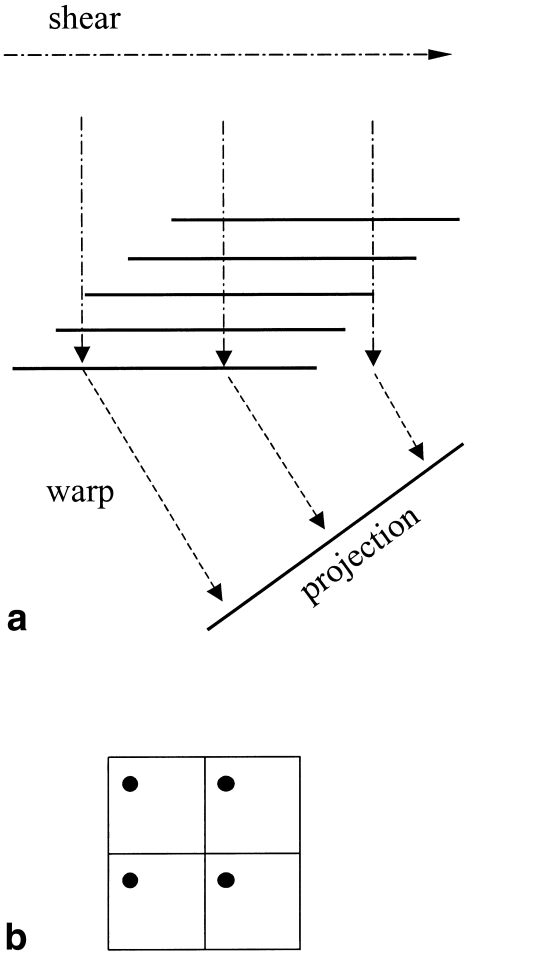

FIG. 2. **a:** Schematics for the shear warp factorization. **b:** Four adjacent square resampling cells in shear warp factorization (dots in cells represent rays). Note that the resampling weighting coefficients determined by the distances from the ray to the four corners are identical for all cells in one slice.

tion for interactive MIP at arbitrary angle or continuous visualization, three copies of data ordered corresponding to the three orthogonal shear axes were created in the initial preparation so that the P-matrix multiplication for all projections in subsequent computations were eliminated.

The amount of resampling within the sheared slices can also be substantially reduced by the fact that the linearly interpolated intensity is always smaller than the maximal intensity among the corner points in a resampling cell (13,14). If the current maximal intensity along a ray is larger than the maximal intensity in a cell immediately following the current cell on the ray, then resampling in that immediate cell can be skipped. This reduced resampling is illustrated in Fig. 3. For a volumetric MRA dataset, bright voxels are sparse and the resampling may be skipped for the majority of the cells in a ray. Therefore, the total computational cost per projection can be further reduced through this reduced resampling method. In our implementation for shear warp, the corner number (0–3) corresponding to the largest element in a cell was stored in the last two bits of the 16 bits address of a corner (typically less than 12 bits are used in MRI) during the preparation stage prior to projection. This preparation eliminated redundant searches for maximal cell values and avoided allocation of additional memory.

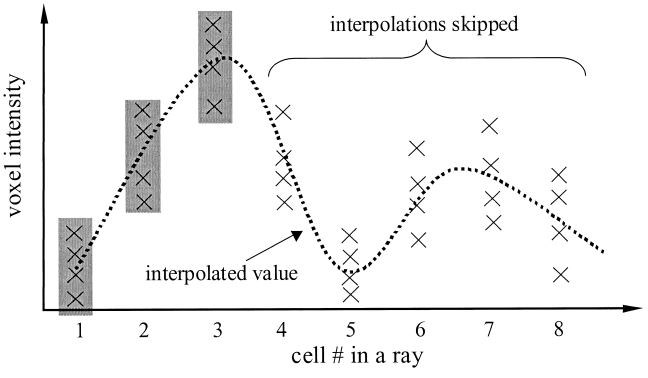

FIG. 3. Reduced resampling in MIP: if the values of all corner points are less than the existing maximum, then the resampling can be skipped (unshaded).

Table 1
Run Time Averaged Over Rotation Angles in [0°, 180°] at 10° Intervals

Time (msec)	Ray casting	Shear warp	Shear warp + reduced resampling
Preparation	0	601	1422
Interpolation + memory access	2100	354	150
Warp	0	15	13
Ray clip	120	0	0
Total (excluding prep)	2220	369	163

For the implementation of the ray casting method, ray clipping that limits resampling to cells in the image volume had to be implemented, which caused additional time. The number of rays varies with the view angle, leading to a ray clip time depending on the view angle.

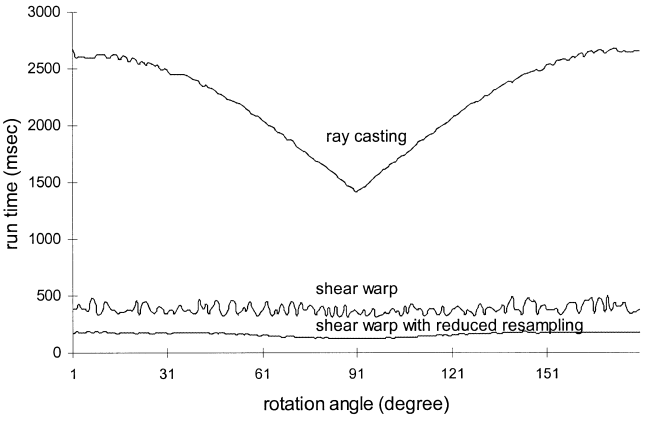

FIG. 4. The run time at different rotation angles. The shear warp reduced the computation time by 6.0 on average compared to the ray casting. The reduced resampling further reduces the computation time by another factor of 2.3 on average.

Experiments and Evaluation

For evaluation, the shear warp methods, with and without reduced resampling, and the ray casting method were implemented using C++ for processing MRA data. To measure the run time of the ray casting and shear warp methods, the program was executed on a PC with ThunderBird 800 MHz CPU (Advanced Micro Devices) with 128 M SDRAM for MIP of various MRA data.

The interpolations in both ray casting and shear warp methods are different and both contain errors. In order to evaluate these errors, a cylindrical object resembling a vessel with 50% diameter stenosis and with intensity known in the continuous coordinate was used to calculate the true projection intensity without any interpolation. Then the object was digitized and corresponding MIP at the same projection angle was performed using ray casting and shear warp methods. The difference between the digital MIP and the true MIP, averaged over the object projection area, was used as an indicator for errors in the interpolation.

RESULTS

The run time result is summarized in Table 1 for a 256 × 256 × 64 dataset. For ray casting, the run time is decomposed into two parts: 1) interpolation + memory access, and 2) ray clip. For shear warp algorithm, the run time is decomposed into three parts: 1) preparation, 2) interpolation + memory access, and 3) warp. The interpolation + memory access time for the ray casting was on average 5.9 (2100/354) times shorter than that for the shear warp. The reduced resampling decreased the interpolation + memory access time by 2.4 (354/150) times on average. The warp time was very small (13–15 msec). The reduced resampling skipped approximately 83% cells in the MRA data used in this study. Shear warp with reduced resampling provided reduction in total run time by 13.6 (2220/163) times on average when compared to ray casting. The shear warp factorization alone reduced the total run time by 6.0 (2220/369) times. The total run time for ray casting varied with the projection angle with a minimal at the 90° projection where the number of rays was minimal (Fig. 4). The anglar dependence of run time was much less obvious for the shear warp methods. Examples of MRA MIP images using both the ray casting and shear warp methods are shown in Fig. 5, showing similar image quality.

The intensity of the test object is shown in a diametric cross section in Fig. 6a and corresponding true MIP is depicted in Fig. 6b. The error maps for both ray casting and shear warp MIPs are depicted in Fig. 6c,d. The average error for the ray casting generated MIP was 11.5% and the average error for the shear warp generated MIP was 9.3%. The ray casting interpolation had a greater error, with

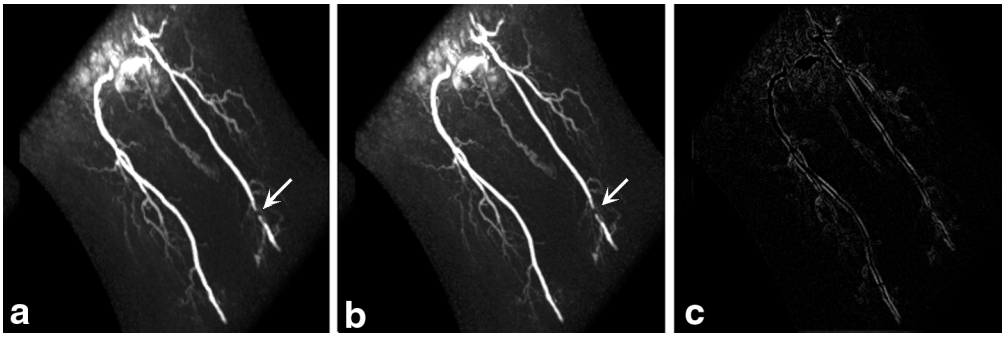

FIG. 5. MIP at (40°, 50°) azimuthal and altitudinal angles using (**a**) ray casting and (**b**) shear warp factorization. Arrows point to a tight occlusion in the left popliteal artery. **c:** The subtraction image between **a** and **b** demonstrates the difference between ray casting and shear warp factorization.

FIG. 6. **a:** Section cut through along the axis of a cylindrical test object with intensity known in both the continuous coordinate and the digitized coordinate. **b:** True MIP image generated from the continuous coordinate without interpolation. **c:** The difference between the true MIP and the ray casting-generated MIP. **d:** The difference between the true MIP and the shear warp generated MIP.

more pronounced error occurred near the edge of the test object (Fig. 6c).

DISCUSSION

Our data demonstrate that the computation for interpolation in projection through a volume dataset is drastically reduced by factorizing the view matrix into a shear warp form. The shear warp form has the following symmetry of reduced computation: the resampling cell size for interpolation is reduced from an 8-corner cubic in ray casting to a 4-corner square in shear warp (cf. Figs. 1b, 2b); furthermore, the weighting coefficients for all cells are identical along one slice in shear warp. A simple 2D warp matrix can restore the aspect ratio from the shear projection with a very small computation time. The shear warp factorization reduces the computation for the linear interpolation by a factor of 5 and, with the additional benefit of fast memory access to data in storage order, achieves a net acceleration in computation by a factor of 6 (Table 1).

For maximal intensity projection, the computation for interpolation can be further reduced by the following property: the interpolated value in a cell is always less than the maximal value among the cell corners. Accordingly, the resampling computation for interpolation can be skipped in a cell where the current maximal value along the projection line is not less than the cell corner maximal. This reduced resampling accelerates the projection by a factor greater than 2 and correspondingly the total reduction in scan time by the fast shear warp algorithm is more than 12-fold (Table 1).

There is a very small cost associated with the shear warp factorization, i.e., to prepare data matrix once prior to computation for projections in all angles. We emphasize that this small cost is one-time only prior to computing projections for all angles and does not add time to real time continuous projections along various angles. In our current implementation of shear warp, this preparation allocated additional memory, which may be an issue if the data size is very large and the computer memory is very limited. This has not been a problem in our study with MRA data on PCs with a standard memory size (128 MB). The reduced resampling for MIP also requires preparation to identify the cell corner maximal, which is also one-time only prior to computation for projections in all angles.

The shear warp factorization not only drastically reduces the redundancy in computation in the ray casting, but also provides a slight improvement in the accuracy of interpolation. There is always error associated with the calculation of interpolation. There are more computation steps and hence more chances for errors in the trilinear interpolation of Eq. [1], as compared with the bilinear interpolation in Eq. [2].

In conclusion, shear warp factorization and reduced resampling drastically increases the speed of MIP.

APPENDIX

We provide here a summary of the basic formulation for the shear warp algorithm (11) for the convenience of readers interested in implementation. Let (X,Y,Z) be the object coordinate and (x,y,z) be the image coordinate. The view matrix M_{view} is defined as:

$$\begin{bmatrix} x \\ y \\ z \\ w \end{bmatrix} = M_{view} \begin{bmatrix} X \\ Y \\ Z \\ W \end{bmatrix}.$$

Here w and W are dummy coordinates allowing translation been accounted in the view matrix. The shear warp algorithm is to factorize the view matrix, multiplied by a matrix P that permutes the axes, into a warp and shear matrices:

$$M_{view}P^{-1} = M_{warp}M_{shear} \equiv [m_{ij}].$$

The shear matrix can be computed from the elements of the permuted view matrix as:

$$M_{shear} = \begin{bmatrix} 1 & 0 & s_a & t_a \\ 0 & 1 & s_b & t_b \\ 0 & 0 & 1 & 0 \\ 0 & 0 & 0 & 1 \end{bmatrix},$$

with s_a, s_b, t_a, t_b calculated as:

$$s_a = \frac{m_{22}m_{13} - m_{12}m_{23}}{m_{11}m_{22} - m_{21}m_{12}}, \; s_b = \frac{m_{11}m_{23} - m_{21}m_{13}}{m_{11}m_{22} - m_{21}m_{12}},$$

$$t_a = (\text{sign}(s_a) - 1)s_aI_{max}, \; t_b = (\text{sign}(s_b) - 1)s_bI_{max},$$

where I_{max} is the maximal slice index in the 3D image volume.

The warp matrix can be computed similarly. Since the warp matrix only operates on the plane of final coordinates (x,y), the 3D version of the warp matrix is simplified to a 2D version of the warp matrix:

$$\begin{bmatrix} x \\ y \\ 1 \end{bmatrix} = M_{warp2D} \begin{bmatrix} x' \\ y' \\ 1 \end{bmatrix}, M_{warp2D} = \begin{bmatrix} m_{11} & m_{12} & m_{14} - t_a m_{11} - t_b m_{12} \\ m_{21} & m_{22} & m_{24} - t_a m_{21} - t_b m_{22} \\ 0 & 0 & 1 \end{bmatrix}.$$

REFERENCES

1. Anderson CM, Saloner D, Tsuruda JS, Shapeero LG, Lee RE. Artifacts in maximum-intensity-projection display of MR angiograms. Am J Roentgenol 1990;154:623–629.
2. Laub G. Displays for MR angiography. Magn Reson Med 1990;14:222–229.
3. Brown DG, Riederer SJ. Contrast-to-noise ratios in maximum intensity projection images. Magn Reson Med 1992;23:130–137.
4. Lin W, Haacke EM, Masaryk TJ, Smith AS. Automated local maximum-intensity projection with three-dimensional vessel tracking. J Magn Reson Imag 1992;2:519–526.
5. Murakami T, Kashiwagi T, Nakamura H, Tsuda K, Azuma M, Tomoda K, Hori S, Kozuka T. Display of MR angiograms: maximum intensity projection versus three-dimensional rendering. Eur J Radiol 1993;17:95–100.
6. Napel S, Marks MP, Rubin GD, Dake MD, McDonnell CH, Song SM, Enzmann DR, Jeffrey RB Jr. CT angiography with spiral CT and maximum intensity projection. Radiology 1992;185:607–610.
7. Levoy M. Display of surfaces from volume data. IEEE computer graphics and applications. 1988;8:29–37.
8. Ylä-Jääski J, Klein F, Kübler O. Fast direct display of volume data for medical diagnosis. CVGIP: Graphic models and image processing. 1991;53:7–18.
9. Yagel R, Kaufman A. Template-based volume viewing. Cambridge, UK: Eurographics 92. p C153–167.
10. Lacroute P, Levoy M. Fast volume rendering using a shear-warp factorization of the viewing transformation. In: Proc SIGGRAPH; 1994. p 451–458. (http://graphics.stanford.edu/papers/shear/shearwarp.pdf)
11. Lacroute P. Fast volume rendering using a shear-warp factorization of the viewing transformation, technical report CSL-TR-95-678. Ph.D. dissertation, Stanford University, 1995. (http://graphics.stanford.edu/papers/lacroute_thesis/)
12. Csebfalvi B, König A, Gröller E. Fast maximum intensity projection using binary shear-warp factorization. Institute of computer graphics and algorithms. Vienna University of Technology, A-1040 Karlsplatz 13/186/2; Technical Report TR-186-2-99-02, January 1999 (http://www.cg.tuwien.ac.at/research/TR/99/TR-186-2-99-02Abstract.html)
13. Sakas G, Grimm M, Savopoulos A. Optimized maximum intensity projection (MIP). In: Proc 6th Eurographics Workshop on Rendering, Dublin, June 1995. (http://www.igd.fhg.de/igd-a7/projects/invivo/papers.html)
14. Erickson BJ, Rettmann DW. A method for rapid computation of maximum intensity projection images. J Digit Imag 1997;10(Suppl 1):207–208.